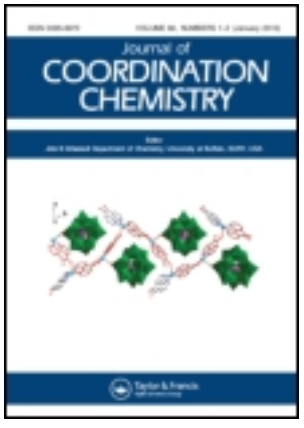

Journal of Coordination Chemistry
Publication details, including instructions for authors and subscription information:
http://www.tandfonline.com/loi/gcoo20

Synthesis, spectral, DFT and X-ray study of a cis-MoO_2 complex with a new isothiosemicarbazone ligand

Reza Takjoo [a], Joel T. Mague [b], Alireza Akbari [c] & Mehdi Ahmadi [c]

[a] Department of Chemistry, School of Sciences, Ferdowsi University of Mashhad, Mashhad, Iran

[b] Department of Chemistry, Tulane University, New Orleans, LA, USA

[c] Department of Chemistry, Payame Noor University (PNU), Tehran, Iran

Accepted author version posted online: 03 Apr 2013.

To cite this article: Reza Takjoo, Joel T. Mague, Alireza Akbari & Mehdi Ahmadi (2013): Synthesis, spectral, DFT and X-ray study of a cis-MoO_2 complex with a new isothiosemicarbazone ligand, Journal of Coordination Chemistry, 66:11, 1854-1865

To link to this article: http://dx.doi.org/10.1080/00958972.2013.791922

Journal of Coordination Chemistry, 2013
http://dx.doi.org/10.1080/00958972.2013.791922

Synthesis, spectral, DFT and X-ray study of a *cis*-MoO_2 complex with a new isothiosemicarbazone ligand

REZA TAKJOO*†, JOEL T. MAGUE‡, ALIREZA AKBARI§ and MEHDI AHMADI§

†Department of Chemistry, School of Sciences, Ferdowsi University of Mashhad, Mashhad, Iran
‡Department of Chemistry, Tulane University, New Orleans, LA, USA
§Department of Chemistry, Payame Noor University (PNU), Tehran, Iran

(*Received 2 July 2012; in final form 6 February 2013*)

2,4-Dihydroxybenzaldehyde *S*-allylisothiosemicarbazone hydrobromide, H_2L, reacts with dioxomolybdenum acetylacetonate in methanol to form a stable complex of dioxomolybdenum(VI). The ligand and complex are characterized with analytical and spectroscopic techniques. Single-crystal X-ray crystallography has been also carried out for the complex, showing it has distorted octahedral geometry. H_2L is a tridentate dianionic ligand bonded as an ONN donor to molybdenum. Thermogravimetric analysis of the complex shows MoO_3 as the final product above 780 °C. The results obtained from density functional theory calculations for the optimization and frequency analysis are in agreement with the experimental data. Natural bond orbital calculations show that the majority of the electron density of the donors tends to the molybdenum, since the calculated Mulliken charge for the central ion is much lesser than the formal value.

Keywords: Isothiosemicarbazone; Molybdenum(VI) complex; TG; Crystal structure; DFT

1. Introduction

Molybdenum is a trace element in nature and plays an important role in metabolism of plants and animals [1, 2]. As potential models for biologically active molybdenum compounds, Schiff base complexes of molybdenum have been used in applications related to catalytic, enzymological and oxygen transfer reactions [3]. Tridentate dibasic Schiff base complexes such as *cis*-$MoO_2L(D)$ (D = solvent) are good substrates for redox reactions because of the ability of D replacement with other solvent [4]. There are a number of crystal structures of molybdenum(VI) complexes of this class in all of which molybdenum coordinates to an *S*-alkyl-isothiosemicarbazone, two oxo ligands and solvent [5].

There is interest in new molybdenum complexes of these types due to the unique properties and potential for biological and catalytic activities. With the X-ray structures, density functional theory (DFT) computations [6] can be carried out to more fully characterize the complexes through calculation of optimized structures, vibrational frequencies and assessment of Natural bond orbitals (NBO's) [7–9].

*Corresponding author. Email: r.takjoo@um.ac.ir

In this article, we have synthesized and characterized a new 2,4-dihydroxybenzaldehyde *S*-allylisothiosemicarbazone hydrobromide (H_2L) and its molybdenum complex *cis*-$MoO_2(L)(MeOH)$ via spectral studies, Thermogravimetric (TG), X-ray and DFT calculations.

2. Experimental

2.1. *Reagents and physical measurements*

All chemicals were of analytical reagent grade and used without purification. Fourier transformation-infrared (FT-IR) spectra were recorded as KBr pellets from 400 to 4000 cm^{-1} on a FT-IR 8400-SHIMADZU spectrophotometer. ^1H NMR spectra were recorded in DMSO-d_6 on a Bruker BRX 100 AVANCE spectrometer. UV–Vis spectra of the compounds were run in methanol on a SHIMADZU model 2550 UV–Vis spectrophotometer, from 210 to 600 nm. Carbon, hydrogen, and nitrogen analyses were carried out using a Thermo Finnigan Flash Elemental Analyzer 1112EA instrument. The molar conductance of 10^{-3} M solution of the metal complex in methanol was measured at room temperature using a Metrohm 712 Conductometer. Thermogravimetric (TG) analysis was carried out by a TGA-50 SHIMADZU under air from 20 to 850 °C with a heating rate of 10 °C min^{-1}. Diffraction data were measured using a Bruker Smart APEX CCD diffractometer.

2.2. *Preparation of 2,4-dihydroxybenzaldehyde S-allylisothiosemicarbazone hydrobromide (H_2L)*

A mixture of allyl bromide (2.66 g, 22 mM) and thiosemicarbazide (2 g, 22 mM) was refluxed in 15 ml ethanol until the solid disappeared (ca. 1 h). 2,4-Dihydroxybenzaldehyde (3.04 g, 22 mM) was added to the solution and the reflux continued for 1 h. After cooling the solution, the yellow precipitate was collected, washed with cold ethanol and dried in vacuum over silica gel.

Yield: 5.2 g, 85%. m.p.: 190 °C. Anal. Calcd for $C_{11}H_{13}BrN_3O_2S$ (331.21 g M^{-1}): C, 39.77; H, 4.25; N, 12.65. Found (%): C, 39.56; H, 4.17; N, 12.51. FT-IR (KBr, cm^{-1}): ν(O4–H) 3,694 w, $\nu_{as}(NH_2)$ 3,250 ms, $\nu_s(NH_2)$ 3,144 ms, ν(O3–H) 3,150 w, ν(C–H) 2,820–2,950 w, $\nu(C{=}C)_{allyl} + \delta CH_2$ 1,650 w, $\delta_{ipb}(O3H) + \delta NH_2 + \nu(C{=}C) + \nu(C1{=}N1)$ 1,627, $\nu(C8{=}N2) + \nu(C{=}C) + \delta NH_2$ 1,581 vs, ν(C5,7-O) 1,157 ms, ν(N–N) 1,060w, δ_{opb}(C–H) 794 mw. ^1H NMR (100 MHz, DMSO-d_6, ppm): 10.4 (s, 1H, O3H); 9 (s, 1H, O4H), 8.4 (s, 1H, CH=N), 7.4 (d, 1H, C4H), 6.4 (d, 1H, C3H), 6.2 (s, 1H, C6H), 5.8 (m, 1H, C10H), 5.2 (d, 2H, $C9H_2$), 4.2 and 3.4 (s, syn/anti:1/1, 2H, NH_2), 3.7 (d, 2H, $C12H_2$). UV–Vis (methanol, λ_{max} (nm), log ε, L M^{-1} cm^{-1}): 240 (4.2), 288 sh (4.19), 300 sh (4.23), 330 (4.46).

2.3. *Preparation of cis-dioxo-methanol-(2,4-dihydroxo-salicylaldehyde S-allylisothiosemicarbazone)molybdenum(VI) (cis-MoO_2(L)(MeOH))*

A methanolic solution (3 ml) of H_2L (0.066 g, 0.2 mM) was added to a solution of dioxomolybdenum acetylacetonate (0.065 g, 0.2 mM) in methanol. The solution was stirred under reflux at 100 °C for 1 h. Red parallelepiped crystals were obtained after two days in a refrigerator. The product was filtered, washed with cool methanol and finally dried in vacuo over $CaCl_2$.

Yield: 0.06 g, 77%. m.p.: 225 °C. Anal. Calcd for $C_{12}H_{15}MoN_3O_5S$ (409.29 g M^{-1}): C, 35.21; H, 3.69; N, 10.28. Found (%): C, 35.45; H, 3.68; N, 10.36. FT-IR (KBr, cm^{-1}): ν(O5H) 3,567 vw, ν(O4H) 3,483 vw, ν(NH) 3,379 m, ν(CH) 2,923–3,068 vw, $\nu(C=C)_{allyl} + \delta CH_2$ 1,640 w, ν(C1=N1) + $\nu(C=C)_{ring}$ + δ(NH) 1,596 vs, ν(C1=N1) + ν(C8=N2) + $\nu(C=C)_{ring}$ 1,550 ms, δ_{ipb}(NH) + ν(C1=N1) + $\nu(C=C)_{ring}$ 1,543 s, ν(C8=N2) + δ_{ipb}(NH) + ν(C1=N1) 1,443 ms, δ_{ipb}(C1H) + δ_{ipb}(N–H) + δ_{ipb}(O4H) 1,287 m, ν(C5,7-O) 1,172 mw, ν(N–N) 1,036 vw, ν_s(*cis*-Mo=$(O)_2$) 942 s, ν_{as}(*cis*-Mo=$(O)_2$) 910 s, δ_{opb}(C–H) 768 m, ν(Mo–O) 609 m, ν(Mo–N) 570 m. ^{1}H NMR (100 MHz, DMSO-d_6, ppm): 12.9 (s, 1H, O5H), 10.3 (s, 1H, NH), 9.8 (s, H, O4H), 8.8 (s, 1H, CH=N), 7.9 (d, 1H, C4H), 6.3 (d, 2H, C3H), 6.2 (s, 1H, C6H), 5.8 (m, 1H, C10H), 5.2 (d, 2H, $C9H_2$), 4 (d, 2H, $C12H_2$), 3.7 (s, 3H, $C11H_3$). UV–Vis (methanol, λ_{max} (nm), log ε, L M^{-1} cm^{-1}): 246 (4.33), 330 (4.39), 332sh (4.26), 440 (3.65). Molar conductivity (1×10^{-3} M L^{-1}; MeOH) 23 Ω^{-1} cm^2 M^{-1}.

2.4. *Theoretical calculations*

The geometry was fully optimized by DFT and all calculations performed using the hybrid B3LYP exchange correlation functional [10]. The calculations were done using the 6-311G**(d,p) [11] basis set for the H, C, N, O and S atoms and Lanl2dz [12] basis set for molybdenum in gas phase by GAUSSIAN 98 [13]. The Mo(VI) complex and H_2L were fully optimized. No symmetry constraints were applied in the calculations. The optimized structures have been used for the frequency calculations. The lack of negative numbers for the frequencies provided evidence for full optimization of the structures. Analysis of the NBO was done by the NBO-code included in Gaussian 98 [14].

2.5. *Structure determination*

A red parallelepiped crystal of the Mo complex, obtained by slow evaporation of a methanolic solution of the complex, was mounted on a Cryoloop® with a film of Paratone® oil and placed in the cold nitrogen stream on the Smart APEX diffractometer. Diffraction data were obtained from three sets of 400 frames, each of width 0.5° in ω, collected at $\varphi = 0.00$, 90.00 and 180.00°, and two sets of 800 frames, each of width 0.45° in φ, collected at $\omega = -30.00$ and 210.00° under control of the APEX2 software package [15]. The scan time was 20 s/frame. The raw data were converted to F^2 values with SAINT [16], which also performed a least-squares optimization of unit cell parameters using 9,840 reflections. Corrections for absorption and merging of equivalent reflections were performed with SADABS [17] and the structure was solved by Patterson and Patterson expansion methods (SHELXS [18]). The structure was refined by full-matrix least squares and hydrogens attached to carbon placed in calculated positions (SHELXL [18]). Hydrogens attached to nitrogen and oxygen were placed in the locations obtained from a difference map and all hydrogens were included as riding contributions with isotropic displacement parameters tied to those of the attached atoms. Other calculations were performed with SHELXTL [19], and the details are presented in table 1.

3. Results and discussion

By using *S*-allylisothiosemicarbazone hydrobromide (H_2L) as ligand and dioxo-molybdenum(VI) acetylacetonate in methanol, *cis*-MoO_2(L)(MeOH) has been synthesized and

Table 1. Crystal, collection and refinement data for *cis*-MoO_2(L)(MeOH).

Chemical formula	$C_{12}H_{15}MoN_3O_5S$
Formula weight	409.27
T/K	100(2)
Crystal system	Monoclinic
Space group	$P2_1/n$
a (Å)	7.5347(8)
b (Å)	18.3928(19)
c (Å)	11.1854(12)
β (°)	107.741(1)
V (Å^3), Z	1476.4(3), 4
Density (g/cm^3)	1.841
μ (mm^{-1})	1.507
F(000)	824
Crystal size (mm)	$0.21\times0.08\times0.05$
θ range for data collection	2.21–29.09°
Index ranges	$-9\leqslant h\leqslant 10,\ -25\leqslant k\leqslant 25,\ -15\leqslant l\leqslant 15$
Refl. coll., max. θ	25,184, 29.10°
Indep. refl.	9,840 ($R_{int}=0.0568$)
Data/restraints/parameters	3,827/0/200
Goodness-of-fit on F^2	1.142
R, wR ($I>2(I)$)	0.0370, 0.0939
R, wR (all data)	0.0416, 0.0967
Max. peak and hole (e/Å^3)	1.15,−0.765

characterized by elemental analysis, solution electrical conductivity, FT-IR, ^{1}H NMR, UV–vis and X-ray crystallography. The single crystal X-ray diffraction study indicates that the ligand is present in its dianionic form. The complex is stable in air and soluble in most common solvents except H_2O and $CHCl_3$. The molar conductivity for the complex in methanol ($23\,\Omega^{-1}\,cm^2\,M^{-1}$) is in agreement with non-electrolyte behavior [20].

3.1. *General optimization*

The crystal structure of the molybdenum(VI) complex has been used as initial geometry for geometry calculation. Unfortunately, attempts to obtain suitable crystals of H_2L were ineffective despite using a variety of solvents. Some important bond lengths and angles of the complex are given in table 2, from which it can be seen that the calculated values are in agreement with experimental ones. The maximum deviation of the calculated structure parameters from the crystal structure is observed for the Mo(1)–O(5) bond (cc. 0.26 Å), but this is for the coordinated methanol, which is the longest (and presumably weakest) bond in the coordination sphere and could be due to steric effects in the crystal packing [21]. For all the structures, vibrational frequency calculations have been done as a check for the optimized structures.

3.2. *Vibrational frequencies analysis*

A number of important vibrational modes of the H_2L and [*cis*-MoO_2(L)(MeOH)] are collected in table 3. Both molecules belong to the C1 symmetry group, and the normal vibrational modes belong to the A1 mode.

Table 2. Selected, calculated, and experimental bond lengths (Å) and angles (°) for *cis*-MoO_2(L)(MeOH) with esd's in parentheses.

Bond type	Exp.	Calcd	Angle type	Exp.	Calcd
Mo1–O2	1.697(3)	1.712	O1–Mo1–O5	82.41(9)	79.51
Mo1–O1	1.722(2)	1.725	O1–Mo1–O3	104.1(1)	105.66
Mo1–O5	2.351(2)	2.612	O1–Mo1–O2	105.7(1)	106.63
Mo1–O3	1.933(2)	1.981	O1–Mo1–N3	96.0(1)	93.71
Mo1–N3	2.038(3)	2.069	N1–Mo1–O5	77.66(9)	74.57
Mo1–N1	2.235(2)	2.282	N1–Mo1–O3	82.1(1)	80.26
C9–S1	1.822(4)	1.852	N1–Mo1–O2	94.5(1)	99.70
C8–S1	1.750(3)	1.773	N1–Mo1–N3	71.2(1)	69.88
C8–N3	1.345(5)	1.350	Mo1–O3–C7	138.7(2)	137.62
C8–N2	1.315(4)	1.304	O3–C7–C2	122.1(3)	122.25
N1–N2	1.410(3)	1.390	C7–C2–C1	123.3(3)	122.77
C1–N1	1.299(4)	1.299	C2–C1–N1	124.8(3)	125.99
C7–O3	1.340(4)	1.322	C1–N1–N2	115.1(3)	115.65
C5–O4	1.361(4)	1.360	N1–N2–C8	108.4(3)	109.49
C1–C2	1.438(4)	1.431	N2–C8–N3	122.6(3)	122.40
C2–C7	1.411(5)	1.421	C8–N3–Mo1	119.5(2)	120.22
C2–C3	1.415(5)	1.412	C8–S1–C9	103.7(2)	102.25
C3–C4	1.374(4)	1.377	S1–C9–C10	106.4(2)	108.96
C4–C5	1.406(5)	1.404	C9–C10–C12	122.8(3)	124.03
C5–C6	1.387(4)	1.390	Mo1–O5–C11	123.9(2)	121.16
C6–C7	1.400(4)	1.400			

The fully optimized structures of the compounds are confirmed by seeing positive values for all calculated frequencies. The calculated frequency values have been multiplied by a suitable scale factor [22] accord with the experimental results. In addition, the calculated and experimental vibrational spectra are given in figure S1 (Supplementary Material). The slight differences between the experimental and computational values indicate appropriate choice of 6-311++G(d,p) hybridization for the calculation. The maximum discrepancies between the experimental and the computational values are in the asymmetric and symmetric stretching modes of NH_2. The asymmetric and symmetric stretching vibrations of NH_2 are at 3,250 and 3,144 cm^{-1} [23] in the experimental spectrum, and at 3,341 and 3,187 cm^{-1} in the computed spectrum. This difference is perhaps due to the lack of interactions in the gas phase computation which would be present in condensed phases. Because of the similarity between IR spectra of the ligand and its Mo(VI) complex from 1,450 to 1,627 cm^{-1} and for better analysis of complex formation, the observed peaks in this region should be individually assigned. Some bending vibrations (scissoring) and in-plane bending of OH, NH, and NH_2 groups appear at 1,500–1,650 cm^{-1} [24, 25]; this can affect other stretching vibrations such as C=C and C=N.

Bands at 1,627, 1,581, and 1,504 cm^{-1} are attributed to, respectively, O3–(H) in-plane bending + aromatic C=C stretching + C1=N1 stretching, C8=N2 stretching + aromatic C=C stretching + NH_2 scissoring and C8=N2 stretching + NH_2 scissoring + C1=N1 stretching. The computed values are 1,596, 1,575, and 1,505 cm^{-1}, respectively.

In the IR spectrum of the molybdenum complex, the O3–H and NH_2 bending modes disappear and the new N3–H bending vibration mixes with the vibration modes of C=C and C=N stretches. Accordingly, bands at 1,596, 1,550, 1,543, and 1,443 cm^{-1} are attributed to, respectively, C1=N1 stretching + aromatic C=C stretching + N3–H in-plane bending, C1=N1 stretching + C8=N2 stretching + aromatic C=C stretching, N3–H in-plane bending + C1=N1 stretching + aromatic C=C stretching and C8=N2 stretching + N3–H in-plane bending + C1=N1 stretching.

Table 3. Selected experimental and calculated IR vibrational frequencies (cm^{-1}) of the ligand and *cis*-MoO_2(L) (MeOH).

Ligand		Complex		
Exp. ν (cm^{-1})[a]	Scaled *v* (cm^{-1})	Exp. *v* (cm^{-1})	Scaled *v* (cm^{-1})	Assignment
486 mw	493	498 w	492	Aromatic C–C–C flipping
N-e	N-e	570 m	562	Mo–N stretching
N-e	N-e	609 m	603	Mo–O stretching
717	770	740 w	732	C8–S1 stretching + N2–C8–N3 scissoring
794 mv	798	768 m	782	Aromatic and azomethine C–H out of plane bending
848 m	867	870 ms	859	Allyl C12, C9–$(H)_2$ rocking
N-e	N-e	910 s	926	*cis*–Mo=$(O)_2$ asymmetric stretching
N-e	N-e	942 s	945	*cis*–Mo=$(O)_2$ symmetric stretching
N-e	N-e	994 w	987	C11–(O) alcohol stretching
1060 w	987	1036 vw	1001	N1–N2 stretching
1143 ms	1146	1064 w	1135	O4–(H) and aromatic C–(H) in plane bending
N-e	N-e	1126 m	1143	N3–(H) and O4–(H) in plane bending
1157 ms	1165	1172 mw	1171	C5, C7–(O) stretching + aromatic C–H and O4–(H) in plane bending
N-e	N-e	1287 m	1312	Azomethine C–H, N3–(H) and O4–(H) in plane bending
1383 m	1426	1409 vw	1420	Allyl C12, C9–$(H)_2$ scissoring
N-e	N-e	1443 ms	1487	C8–N2 and C1=N1 stretching + N3–(H) in plane bending
N-e	N-e	1543 s	1524	N3–(H) in plane bending + C1=N1 and aromatic C=C stretching
1504 ms	1505	N-e	N-e	C8=N2 and C1=N1 stretching + NH_2 scissoring
N-e	N-e	1550 ms	1571	C1=N1, C8=N2 and aromatic C=C stretching
N-e	N-e	1596 vs	1579	C1=N1 and aromatic C=C stretching + N3–(H) in plane bending
1581 vs	1575	N-e	N-e	C1=N1, C8=N2 and aromatic C=C stretching + NH_2 scissoring
1627 vs	1596	N-e	N-e	O3–(H) in plane bending + aromatic C=C, C1=N1 stretching
N-e	N-e	2908 w	2898	C11–$(H)_3$ alcohol symmetric stretching
N-a	2916–3024	2950–3168 vw	2950–3169	Allyl, azomethine C–(H) stretching
N-e	N-e	3050 w	3027	C11–$(H)_3$ alcohol asymmetric stretching
2820–2950 w	3157–3190	2923–3068 vw	3042–3178	Aromatic C–(H) stretching
3150 w	3066	N-e	N-e	O3–(H) stretching
3144 ms	3187	N-e	N-e	NH_2 symmetric stretching
N-e	N-e	3379 m	3448	N3–(H) stretching
3250 ms	3341	N-e	N-e	NH_2 asymmetric stretching
3694 w	3634	3483 vw	3672	O4–(H) stretching
N-e	N-e	3567 vw	3683	O5–(H) alcohol stretching

[a]Wavenumber.
Abbreviations: vs: very strong; s: strong; ms: medium strong; m: medium; w: weak; vw: very weak; N-e: Inactive.

By ignoring the bending vibrations of O3–(H) and NH_2 in the infrared spectrum of the ligand, and disregarding the N3–(H) bend in the IR spectrum of the molybdenum complex, we would see the stretch of C=N1 at 1,627 and 1,581 cm^{-1} in H_2L red shifting to 1,596 and 1,550 cm^{-1} in the complex. These indicate coordination of the ligand through the azomethinic nitrogen (N1) [26].

The absence of $\nu_{as}(NH_2)$ and $\nu_s(NH_2)$ in the IR spectrum of the complex also confirms that the ligand is coordinated by deprotonated thioamide nitrogen (N3).

The C–H stretch of the methyl of coordinated methanol is at 2,908–3,050 cm^{-1} in the experimental spectrum and 2,898–3,027 cm^{-1} in the computed spectrum [26]. The C–O stretch is at 1,157 cm^{-1} in the infrared spectrum of the free ligand, shifting to lower frequency by 15 cm^{-1} upon coordination (1,172 cm^{-1}). These values are computed at 1,165 and 1,171 cm^{-1} for the ligand and complex, respectively. Very weak peaks at 3,567 and 994 cm^{-1} for the Mo(VI) complex are related to stretching vibration of O5–H and C11–O5 of coordinated methanol [27] which are calculated at 3,683 and 987 cm^{-1}.

The symmetric and anti-symmetric stretching vibrations of O=Mo=O are at 910 and 942 cm^{-1} as two distinct peaks with calculated values at 926 and 945 cm^{-1}, respectively [28]. The existence of two bands with the same intensity reveals *cis* oxygens [29].

3.3. *Electronic charge distribution*

The HOMO and LUMO of the complex are given in figure 1. The HOMO is located predominantly on the donors and the LUMO is located on molybdenum. The calculated partial electronic charges (Mulliken analysis) of participating atoms in bonding are collected in table S1. The data show that N3 and O3 have Mulliken values less than the formal charge of −1. Calculated charge values for O1 and O2 are −0.639 and −0.634 a.u., respectively, less than the formal charge −2 expected for oxides. The calculated value of 0.050 a.u. for N1 indicates that this nitrogen gives an electron pair to molybdenum and does not contribute negative charge to the system. These results together with the 2.331 a.u. charge on molybdenum, in comparison with the expected formal charge (+6), indicate that most of the donor atoms transmit electron density to molybdenum [30]. For bond formation, Mo, N- and O-donors of the ligand use 5s and 4d orbitals, 2s and 2p orbitals, respectively.

Additional NBO data are given in table 4. According to the NBO calculations for *cis*-MoO_2, there are four σ and π bonding orbitals, and four σ^* and π^* antibonding orbitals. The bonding orbitals are filled whereas the remainder are empty. The σ bonding orbitals of {Mo=O} are mainly polarized toward O1 and O2 (respectively 74.5 and 73.99%). In these bonds, molybdenum uses the 5s and 4d valence bonding orbitals and the 2s and 2p valence orbitals are used by oxygens (O1, O2). The π bonding electrons are polarized by 68.04 and 68.52% toward O1 and O2, respectively. For formation of the π bond, molybde-

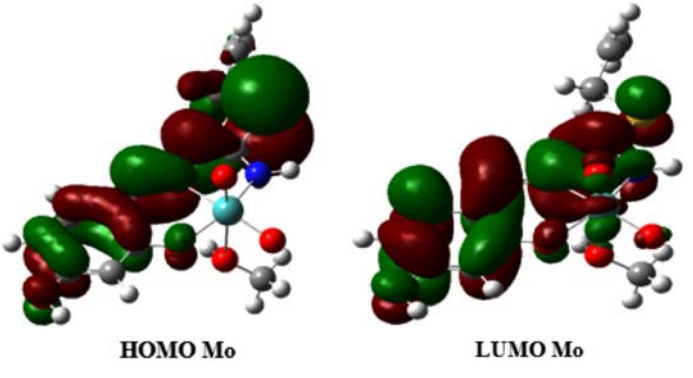

Figure 1. HOMO and LUMO for *cis*-MoO_2(L)(MeOH).

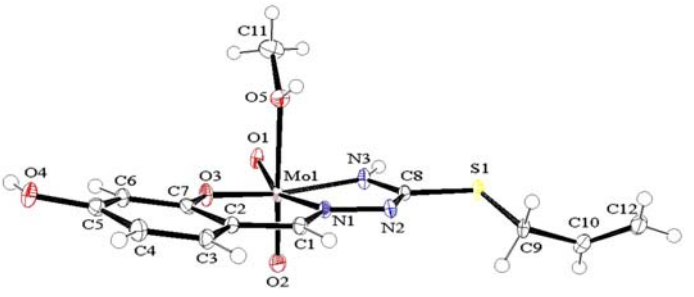

Figure 2. ORTEP drawing of *cis*-MoO$_2$(L)(MeOH) with atom numbering. Thermal ellipsoids are shown at the 50% probability level.

Table 4. The occupancy, hybrids and coefficient for the *cis*-MoO$_2$ unit.

Bond	Bond type	Coefficients	Percentage	Hybrids	Occupancy
Mo(1)–O(1)	σ	0.5045 Mo	25.45	$s^{16.87}d^{82.61}$	1.96260
		0.8634 O	74.55	$s^{22.60}p^{77.32}$	
Mo(1)–O(1)	π	0.5653*Mo	31.96	$d^{98.84}$	1.965
		0.8249*O	68.04	$p^{99.93}$	
Mo(1)–O(2)	σ	0.5100*Mo	26.01	$s^{19.4}d^{79.89}$	1.95320
		0.8602*O	73.99	$s^{21.5}p^{78.41}$	
Mo(1)–O(2)	π	0.5611*Mo	31.48	$d^{99.79}$	1.95320
		0.8278*O	68.52	$P^{99.78}$	
Mo(1)–O(1)	σ*	0.8634*Mo	74.55	$s^{16.87}d^{82.61}$	0.25559
		−0.5045*O	25.45	$s^{22.60}p^{77.32}$	
Mo(1)–O(1)	π*	0.8249*Mo	68.04	$d^{98.84}$	0.23116
		−0.5653*O	31.96	$p^{99.93}$	
Mo(1)–O(2)	σ*	0.8602*Mo	73.99	$s^{19.46}d^{79.89}$	0.20198
		−0.5100*O	26.01	$s^{21.50}p^{78.41}$	
Mo(1)–O(2)	π*	0.8278*Mo	68.52	$d^{99.79}$	0.25428
		−0.5611*O	31.48	$p^{99.78}$	

num and oxygen use d and p orbitals, respectively. According to table 4, the σ* and π* antibonding orbitals are polarized toward molybdenum.

3.4. *^{1}H NMR and electronic spectra*

Scheme 1 shows the numbering of the ligand and the ORTEP drawing of the Mo(VI) complex is used to assign of the proton resonances. In the ^{1}H NMR spectrum of the ligand, the O4H and O3H appear at 10.4 and 9 ppm, respectively. After complexation O3H resonance disappears, indicating coordination occurs through the deprotonated oxygen. The azomethine proton (CH=N) at 8.4 ppm in the spectrum of the ligand shifts to 8.8 ppm after coordination, confirming that N1 coordinates to Mo. The presence of the isothiosemicarbazone in *Z* and *E* (scheme 1) configurations in the solution is well known [31]. In the *E* isomer, S–R lies *trans* to N1 while in the *Z* isomer they are *cis* (scheme 1) [32, 33]. The existence of both tautomeric structures in solution is confirmed by the presence of two signals for NH$_2$ at 4.2 and 3.4 ppm and only one set of coupling constants and chemical shifts are observed for other protons in the ligand. The appearance of a new broad singlet at 10.3 ppm related to N3H with omission of the NH$_2$ signals in the ^{1}H NMR of the complex

shows coordination of the deprotonated thioamide nitrogen. Two signals of CH_3 and O5H of coordinated methanol are revealed at 3.7 and 12.9 ppm, respectively. The position of these bands confirm that methanol is not coordinated to molybdenum in the presence of DMSO.

Electronic absorption data of the ligand and the Mo-complex are summarized in Sections 2.2 and 2.3. The UV–vis spectra are given in figure S2. The spectrum of H_2L has two bands at 240 (4.2) and 288 nm (4.19) which are attributed to $\pi \rightarrow \pi^*$ transitions of the aromatic ring and the azomethine, respectively. Bands at 300 (4.23) and 330 nm (4.46) are attributed to $n \rightarrow \pi^*$ transitions of the azomethine and thioamide, respectively [34]. In the electronic spectrum of the complex, the band at 246 nm (4.33) is assigned to $\pi \rightarrow \pi^*$ transition of the aromatic ring, whereas the $n \rightarrow \pi^*$ transition of azomethine and thioamide are at 330 nm (4.39). The complex also exhibits a band at 440 nm (3.65), due to $N \rightarrow Mo(VI)$ and $O \rightarrow Mo(VI)$ (LMCT) charge-transfer transitions. These transitions would be from the p-orbital of the ligand to the lowest empty molybdenum d-orbitals [35].

3.5. *Thermal studies*

The TG and differential TG analyses of the Mo-complex have been determined to 1,000 °C using a heating rate of 10 °C min^{-1}. Figure S3 gives the thermal analysis curve of the complex. The compound is stable to 125 °C, then its decomposition occurs in five steps. In the first step, loss of the coordinated methanol occurs at 127–150 °C with a weight loss of 7.83% (calcd 7.7%). The second step takes place by mass loss of 3.92% (calcd 3.9%) from 228 to 243 °C. A NH fragment separates from the residue. In a broader temperature range, from 244 to 426 °C, the third decomposition corresponds to loss of an allyl with a weight decrease of 11.19% (calcd 11.4%). The fourth weight loss of 41.54% (calcd 40.8%) takes place from 430 to 625 °C, corresponding to a fragment, which is probably HOPh(O)C(S)=N. The ultimate residue with 29.98% (calcd 30%) weight, probably MoO_3, can be seen above 780 °C.

3.6. *Crystallography*

Table 1 lists the crystal data and structure refinement results, while an ORTEP view of the compound with the atom numbering is shown in figure 2; pertinent bond distances and inter-bond angles appear in table 2. The coordination geometry can be described as distorted octahedral with bond angles at molybdenum varying from 71.2(1)° to 105.7(1)° (table 2). The angle between the oxo ligands (O1–Mo1–O2) is the largest. While bending O1 away from O2 and out of the equatorial "plane" could be attributed to the strong hydrogen bond with the phenolic –OH in a neighboring molecule at $1-x$, $2-y$, $1-z$ (table 5), this geometry must be largely electronic in origin, since this angle is also calculated to be the largest (table 2). The coordination sphere has *mer* configuration with the tridentate Schiff base coordinated in the *syn* conformation through the anionic phenol

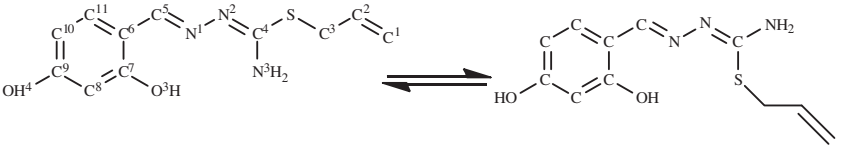

Scheme 1. General structures of the isothiosemicarbazone; (a) *E* and (b) *Z*.

Table 5. Hydrogen bonds for *cis*-MoO_2(L)(MeOH) [Å and °].

D–H···A	d(D–H)	d(H···A)	d(D···A)	∠(DHA)
O4–H4···O1[a]	0.84	1.89	2.725(3)	179
O5–H5O···N2[b]	0.84	1.88	2.722(4)	176
N3–H3 N···O4[c]	0.88	2.33	3.168(4)	159
C9–H9B···cg[d]	0.99	2.78	3.70	155

Symmetry transformations used to generate equivalent atoms: [a]$-x+1, -y+2, -z+1$; [b]$-x+2, -y+2, -z+2$; [c]$-x+3/2, y-1/2, -z+3/2$; [d]cg is the centroid of the ring C2–C9 at $1-x, 2-y, 2-z$.

oxygen, the neutral azomethine nitrogen and the anionic thioamide nitrogen forming one unit and the two oxo ligands and the coordinated methanol the other. The ligand shows a slight concave distortion from planarity in the direction of the coordinated methanol, as indicated by the dihedral angle of 12.3(1)° between the mean planes of the aromatic ring and the N1, N2, C8, N3 portion of the ligand backbone. The Mo=O distances differ significantly with that involving O1, which forms a strong hydrogen bond, being longer. We attribute the lengthening to the hydrogen bonding interaction as the calculated Mo1–O1 distance, which does not involve hydrogen bonding, essentially the same as the Mo1–O2 distance. Similar differences in the two Mo=O bond lengths are seen in a variety of analogous complexes of closely related Schiff base ligands, although in a number of cases the difference is smaller than that found here [5]. The difference in *trans* influences of the central nitrogen of the Schiff base and methanol with the former being the better donor could also be important. The hydrogen bonding interactions O5–H5···N2 and O4–H4···O1 (table 5) create a 1-D chain of bilayers along 101 which are then weakly associated, approximately, along *b* via a C–H···π interaction between C9–H9b, and the centroid of the aromatic ring containing C2–C9 in the molecule at $1-x, 2-y, 2-z$.

4. Conclusion

We have prepared red crystalline *cis*-MoO_2(L)(MeOH) by reaction of 2,4-dihydroxybenzaldehyde *S*-allylisothiosemicarbazone hydrobromide (H_2L) with $MoO_2(acac)_2$ in methanol. The X-ray crystal structure shows a distorted octahedral coordination that possesses the *mer* conformation. The ligand is a dinegative tridentate chelate in its deprotonated form and coordinates to the metal via the azomethine nitrogen, the thioamide nitrogen and the phenolate oxygen. Two oxo ligands and a methanol occupy the remaining coordination sites.

The thermal stability of the complex is low with methanol being removed first and the last step forming MoO_3. Comparison of the vibrational frequencies calculated by DFT methods with the experimental results showed satisfactory agreement and allowed assignments of many bands in the infrared spectra. NBO analysis indicated that the HOMO and LUMO were located on the donor atoms and molybdenum, respectively.

Supplementary data

Full crystallographic data (CCDC No. 871938) for the complex has been deposited at the Cambridge Crystallographic Data Center and are available on request from the Director,

CCDC, 12 Union Road, Cambridge, CB2 1EZ, UK (Fax: +44-1223-336,033; E-mail: deposit@ccdc.cam.ac.uk or http://www.ccdc.cam.ac.uk). The cartesian coordinates of compounds, figures S1, S2, S3, and table S1 are presented in supplementary materials.

Acknowledgements

We would like to appreciate the Tulane Crystallography Laboratory of Chemistry Department, Tulane University, for their invaluable help. Also, we are thankful of Ferdowsi University of Mashhad and Payame Noor University (PNU) for their support.

References

[1] L. Xu, B. Lehmann, J. Mao, T.F. Nägler, N. Neubert, M.E. Böttcher, P. Escher. *Chem. Geol.*, **318**, 45 (2012).
[2] E.A. Smail, E.A. Webb, R.P. Franks, K.W. Bruland, S.A. Sañudo-Wilhelmy. *Environ. Sci. Technol.*, **46**, 4304 (2012).
[3] (a) C. Bibal, J.-C. Daran, S. Deroover, R. Poli. *Polyhedron*, **29**, 639 (2010); (b) G. Romanelli, J.C. Autino, P. Vázquez, L. Pizzio, M. Blanco, C. Cáceres. *Appl. Catal., A*, **352**, 208 (2009); (c) M. Bagherzadeh, M. Amini, H. Parastar, M. Jalali-Heravi, A. Ellern, L.K. Woo. *Inorg. Chem. Commun.*, **20**, 86 (2012).
[4] (a) Y. Sui, X. Zeng, X. Fang, X. Fu, Y. Xiao, L. Chen, M. Li, S. Cheng. *J. Mol. Catal. A: Chem.*, **270**, 61 (2007); (b) N.K. Ngan, K.M. Lo, C.S.R. Wong. *Polyhedron*, **33**, 235 (2012); (c) V.W.L. Ng, M.K. Taylor, C. G. Young. *Inorg. Chem.*, **51**, 3202 (2012).
[5] (a) B.I. Ceylan, Y.D. Kurt, B. Ülküseven. *J. Coord. Chem.*, **62**, 757 (2009); (b) S. Duman, İ. Kızılcıklı, A. Koca, M. Akkurt, B. Ülküseven. *Polyhedron*, **29**, 2924 (2010); (c) A.B. Ilyukhin, V.L. Abramenko, V.S. Sergienko. *Koord. Khim. (Russ.) (Coord. Chem.)*, **25**, 510 (1999); (d) Y.D. Kurt, G.S. Pozan, İ. Kızılcıklı, B. Ülküseven. *Koord. Khim. (Russ.) (Coord. Chem.)*, **33**, 858 (2007); (e) Z.D. Tomić, A. Kapor, A. Žmirić, V. M. Leovac, D. Zobel, S.D. Zarić. *Inorg. Chim. Acta*, **360**, 2197 (2007).
[6] P. Hohenberg, W. Kohn. *Phys. Rev.*, **136**, 864 (1964).
[7] (a) R. Takjoo, R. Centore, M. Hakimi, S.A. Beyramabadi, A. Morsali. *Inorg. Chim. Acta*, **371**, 36 (2011); (b) R. Takjoo, R. Centore. *J. Mol. Struct.*, **1031**, 180 (2013); (c) R. Takjoo, S.W. Ng, E.R.T. Tiekink. *Acta Cryst.*, **E68**, m944 (2012).
[8] S. Roy, T.K. Mondal, P. Mitra, E. Lopez Torres, C. Sinha. *Polyhedron*, **30**, 913 (2011).
[9] S. Michalik. *J. Coord. Chem.*, **65**, 1189 (2012).
[10] A.D. Becke. *J. Chem. Phys.*, **98**, 5648 (1993).
[11] J.S. Binkley, J.A. Pople, W.J. Hehre. *J. Am. Chem. Soc.*, **102**, 939 (1980).
[12] (a) T.H. Dunning, P.J. Hay, H.F. Schaefer. In *Modern Theoretical Chemistry*, Vol. 3, 3rd Edn, p. 1, Plenum Press, New York (1976); (b) P.J. Hay, W.R. Wadt. *J. Chem. Phys.*, **82**, 299 (1985); (c) P.J. Hay, W.R. Wadt. *J. Chem. Phys.*, **82**, 270 (1985).
[13] M.J. Frisch, G.W. Trucks, H.B. Schlegel, G.E. Scuseria, M.A. Robb, J.R. Cheeseman, V.G. Zakrzewski, J.A. Montgomery, Jr., R.E. Stratmann, J.C. Burant, S. Dapprich, J.M. Millam, A.D. Daniels, K.N. Kudin, M.C. Strain, O. Farkas, J. Tomasi, V. Barone, M. Cossi, R. Cammi, B. Mennucci, C. Pomelli, C. Adamo, S. Clifford, J. Ochterski, G.A. Petersson, P.Y. Ayala, Q. Cui, K. Morokuma, D.K. Malick, A.D. Rabuck, K. Raghavachari, J.B. Foresman, J. Cioslowski, J.V. Ortiz, B.B. Stefanov, G. Liu, A. Liashenko, P. Piskorz, I. Komaromi, R. Gomperts, R.L. Martin, D.J. Fox, T. Keith, M.A. Al-Laham, C.Y. Peng, A. Nanayakkara, C. Gonzalez, M. Challacombe, P.M.W. Gill, B. Johnson, W. Chen, M.W. Wong, J.L. Andres, C. Gonzalez, M. Head-Gordon, E.S. Replogle, J.A. Pople. *Gaussian 98,* Revision A.7; Gaussian, Inc.: Pittsburgh, PA, (1998).
[14] E. Reed, L.A. Curtiss, F. Weinhold. *Chem. Rev.*, **88**, 899 (1988).
[15] Bruker-AXS. *APEX2 (Version 2010.11-3)*, Madison, WI (2010).
[16] Bruker-AXS. *SAINT (Version 7.68A)*, Madison, WI (2009).
[17] G.M. Sheldrick. *SADABS (Version 2008/2)*, University of Göttingen, Germany (2008).
[18] G.M. Sheldrick. *SHELXS and SHELXL, Acta Cryst. A*, **64**, 112 (2008).
[19] Bruker-AXS. *SHELXTL (Version 2008/4)*, Madison, WI (2008).
[20] V. Jevtovic, D. Vidovic. *J. Chem. Crystallogr.*, **40**, 794 (2010).
[21] B. Machura, R. Kruszynski, J. Mrozinski, J. Kusz. *Polyhedron*, **27**, 1739 (2008).
[22] J.P. Merrick, D. Moran, L. Radom. *J. Phys. Chem. A*, **111**, 11683 (2007).
[23] N. Ozdemir, M. Shahin, T. Bal-Demirci, B. Ulkuseven. *Polyhedron*, **30**, 515 (2011).

[24] R.M. Silverstein, G.C. Basseler, C. Morill. *Spectrometric Identification of Organic Compounds*, Wiley, New York (1981).
[25] A. Zulfikaroglu, C.Y. Ataol, H. Bati, O. Buyukgungor. *J. Coord. Chem.*, **65**, 1525 (2012).
[26] P. Chinna Babu, N. Sundaraganesan, O. Dereli, E. Turkkan. *Spectrochim. Acta, Part A*, **79**, 562 (2011).
[27] Z.D. Tomic, A. Kapor, A. Zmiric, V.M. Leovac, D. Zobel, S.D. Zaric. *Inorg. Chim. Acta*, **360**, 2197 (2007).
[28] R. Takjoo, M. Ahmadi, A. Akbari, H.A. Rudbari, F. Nicolo. *J. Coord. Chem.*, **65**, 3403 (2012).
[29] A. Syamal, M.M. Singh, D. Kumar. *React. Funct. Polym.*, **39**, 27 (1999).
[30] B. Machura, A. Switlicka, M. Wolffa, J. Kusz, R. Kruszynski. *Polyhedron*, **28**, 1348 (2009).
[31] M. Shahin, T. Bal-Demirci, G. Pozan-Soylu, B. Ulkuseven. *Inorg. Chim. Acta*, **362**, 2407 (2009).
[32] N.V. Gerbeleu, V.B. Arion, J. Burgess. *Template Synthesis of Macrocyclic Compounds*, pp. 38–60, Wiley-VCH, Weinheim (1999).
[33] Y. Kurt, A. Koca, M. Akkurt, B. Ülküseven. *Inorg. Chim. Acta*, **388**, 148 (2012).
[34] Bİ. Ceylan, Y.D. Kurt, B. Ülküseven. *J. Coord. Chem.*, **62**, 757 (2009).
[35] R. Garg, M.K. Saini, N.T. Fahmi, R.V. Singh. *Trans. Metal Chem.*, **31**, 362 (2006).